RSC Advances

PAPER

Cite this: *RSC Adv.*, 2016, **6**, 77465

Development of multilayer Sn–Ni alloy coating by pulsed sonoelectrolysis for enhanced corrosion protection

Sandhya Shetty, M. Mohamed Jaffer Sadiq, D. Krishna Bhat and A. Chitharanjan Hegde*

Multilayer Sn–Ni alloy coating has been developed electrochemically on mild steel using an ultrasound effect, as a tool to modulate mass transfer process at electrical double layer, during deposition. Sn–Ni coatings having alternate layers of alloys of different compositions were developed on a nano/micrometric scale by pulsing sonicator ON (t_{ON}) and OFF (t_{OFF}), periodically. The composition modulated multilayer alloy (CMMA) Sn–Ni coatings have been deposited by inducing the ultrasound field periodically at optimal current density. Corrosion performances of ultrasound-assisted multilayer Sn–Ni alloy coatings have been evaluated by electrochemical methods. Corrosion data revealed that CMMA Sn–Ni coating, developed using pulsed ultrasonic field and having 150 layers, represented as $(Sn–Ni)_{2/2/150}$, is the most corrosion resistant, compared to its monolayer alloy coatings developed by both with/without ultrasound effect. Corrosion protection efficacy of multilayer coatings was found to be decreased at high degree of layering due to diffusion of layers. Improved corrosion resistance of multilayer Sn–Ni coatings is attributed to an increase in the number of layers, or interfaces separating alloys of the same metals, but of different composition, surface morphologies and phase structures, supported by energy dispersive spectroscopy, field emission scanning electron microscopy and X-ray diffraction study, respectively. The better corrosion protection of CMMA Sn–Ni coatings, compared to monolayer counterparts, is attributed to an increase in the number of layers, hence phase boundaries between layers, and experimental results are discussed.

Received 23rd May 2016
Accepted 30th July 2016

DOI: 10.1039/c6ra13302a

www.rsc.org/advances

1. Introduction

A new class of materials with alternate layers of metals/alloys, having a thickness of a few nanometers with ultrafine microstructure, is known as composition-modulated multilayer alloys (CMMA).[1] The concept of CMMA coating is relatively new and is gaining interest amongst researchers, because these layered coatings possess improved properties, such as increased strength, micro-hardness, wear and corrosion resistance, and electrical and magnetic properties.[2] There are different methods for producing multilayer alloy coatings: (i) dry, or vacuum, method, like physical vapour deposition, chemical vapour deposition *etc.*, and (ii) wet, or electrodeposition, method. In the electrodeposition method, CMMA coatings can be obtained by using either a single-bath technique (SBT), where deposition takes place in a plating solution containing ions of the alloy components, or a double-bath technique, where deposition is carried out from separate plating baths by using manual/automated transfer of the substrate from one bath to another. Both techniques are known to have their own advantages and disadvantages.[3,4] Generally, in the SBT,[5–7] the metal ions required to form both deposit layers are contained in a single electrolyte, and alloy deposition is achieved by modulating alternately the mass transport process at electrical double layer (EDL). Such modulation in mass transport process at EDL can be accomplished by changing alternately the cathodic current/potential, magnetic field, ultrasound field, and even temperature, during deposition.[5–9] Actually during electrodeposition, modulation of mass-transfer process brings an increase in the limiting current (i_L) of the more noble metal, which consequently modifies the composition of the alloy to be deposited on the cathode. When an electrolyte with the optimum concentrations of metals is used, the concentration of noble metal ion in the electrolyte is required to be lower than that of the less noble one. In other words, if the ratio of [more noble metal] and [less noble metal] is very small, then obviously the more noble metal will be deposited at low current density (c.d.), and the less noble metal is deposited at high c.d. Therefore, for all practical purposes the SBT can only produce composition-modulated layers of alloys rather than pure metallic layers.

A well-tried method for development of multilayer coatings through the SBT is by changing alternately the cathodic c.d., *i.e.*,

Department of Chemistry, National Institute of Technology Karnataka, Srinivasnagar-575025, Surathkal, India. E-mail: acrhegde@gmail.com

c.d. is made to change alternately between two values at regular time intervals, depending on the requirement of composition and thickness of alternate layers. In this direction there are several reports on development of multilayer alloy coatings for improved corrosion protection of mild steel, in place of their monolayer (monolithic) alloy coating developed using direct current (DC). Among them are the papers of our group[10–15] focused on development of corrosion-protective CMMA coatings of Zn–M (where M = Ni, Co and Fe) alloys by pulsing the c.d., in different patterns, namely square and triangular shape. The coating configurations, in terms of pulsing c.d. and number of layers, have been optimized to maximize their corrosion performance.

Ultrasound is a form of mechanical energy, *i.e.* it is not absorbed by molecules. Ultrasound is transmitted through a medium *via* waves by inducing vibrational motion of the molecules which alternately compress and stretch the molecular structure of the medium. Therefore, the distances between the molecules vary as the molecules oscillate about their mean position. If the intensity of ultrasound in a liquid is increased, a point is reached at which the intramolecular forces are not able to hold the molecular structure intact. Consequently, it breaks down and cavitation bubbles are created.[16] Thus, when ultrasound is applied to liquid media, a range of processes occur which can create unusual physical and chemical conditions; these include acoustic steaming, turbulent convection, microstreaming in the presence of oscillating bubbles and cavitation.[17] At sufficiently high power density (p.d.), when cavities collapse in succeeding compression cycles, the energy generated will bring about many chemical and mechanical effects. This remarkable phenomenon is induced throughout the liquid at ultrasonic frequencies, *i.e.* 20 kHz or above.[18,19] Due to this effect of ultrasound, recently electrodeposition with an ultrasound effect has become a hot topic in the surface engineering field. Further, it can be used to modulate the mass transport process towards the cathode, and to develop multilayer coatings of alloys from electrolytic solutions having metal ions.

Thus, though there are many reports in the literature on both ultrasound-induced electrodeposition (sonoelectrolysis) of many metals/alloys and multilayer Zn-based alloy coatings for better corrosion protection, to the best of the authors' knowledge development of multilayer alloy coatings using the ultrasound effect as a tool is not available. On the other hand, there are many reports on electrodeposition of corrosion-protective coatings of Sn–Ni alloy,[20,21] but no reports on its multilayer coatings are available. Hence to fill this knowledge gap, development of ultrasound-assisted multilayer Sn–Ni alloy coating for better corrosion resistance has been tried. The corrosion performance of sonoelectrodeposited multilayer Sn–Ni alloy coatings was evaluated in relation to its monolayer (conventional) electrodeposits, plated with/without the use of the ultrasound effect. The first part of the paper details the optimization of conditions for development of sonoelectrodeposited monolayer Sn–Ni alloy coating, whilst the second part discusses the optimization of deposition conditions for development of its multilayer coatings for better corrosion protection, using the sonication effect.

2. Experimental

The composition and conditions of the Sn–Ni alloy bath, used throughout the study, are given in Table 1. The optimal conditions in terms of both composition and operating variables, like c.d. and pH, were arrived at by the standard Hull cell method.[3]

The electrolytes were freshly prepared from distilled water using analytical grade reagents. Polished mild steel (MS) plates (0.063% C, 0.23% Mn, 0.03% S, 0.011% P, 99.6% Fe), with an exposed surface area of 7.5 cm^2, served as a cathode, and the anode used was pure nickel plate with the same exposed area. The depositions were carried out in a rectangular PVC cell containing 250 mL electrolyte, maintained at constant temperature (298 K). The pH of the bath was adjusted to 8.6 using either 10% NH_4OH or 10% HCl before each electrodeposition. The MS panels were mechanically mirror polished, degreased by trichloroethylene and then rinsed with distilled water, ultrasonically cleaned in acetone for 10 min, dipped in acid (10% HCl) and finally washed with distilled water before deposition. All electrodepositions were carried out on a known surface area of the cathode. The Ni anode was activated by dipping for a few seconds in 10% HNO_3 before each experiment. The primary additive, namely gelatin, was dissolved in hot water (being insoluble in cold water) and added into the bath to impart a lustrous appearance to the coating.

2.1 Development of monolayer and multilayer Sn–Ni alloy coating

Electrodepositions of monolayer Sn–Ni alloy coating, both in the presence and absence of the ultrasound effect, have been carried out, and deposition conditions were optimized for coatings of maximum corrosion protection. The electrodeposition was carried out using constant current or DC power source (DC Power Analyzer, Agilent Technologies, USA, model: N6705), and sonoelectrodeposition was carried out using an ultrasound generator (SONIC Vibra-Cell™ VC 750, 20 kHz, maximum power 750 W, having sonicator probe (electrode) of 13 mm tip diameter), coupled with DC source. CMMA Sn–Ni coatings were developed in layers by turning the ultrasound generator ON (t_{ON}) and OFF (t_{OFF}) periodically, during DC deposition. The ultrasonic horn was kept at a distance of 1 cm from the cathode during sonoelectrodeposition. The process assembly used for sonoelectrodeposition is shown in Fig. 1.

Multilayer Sn–Ni alloy coatings, having nano/micrometric layers of alloys (with alternately different compositions), were

Table 1 Composition and operating parameters of optimized Sn–Ni bath

Bath constituents	Amount (g L^{-1})	Operating parameters
$SnCl_2 \cdot 2H_2O$	22.6	Anode: pure Ni
$NiCl_2 \cdot 6H_2O$	33.7	Cathode: mild steel (MS)
$K_4P_2O_7$	119	pH: 8.6
Gelatin	5.0	Temperature: 298 K
		Current density: 1.0 A dm^{-2}

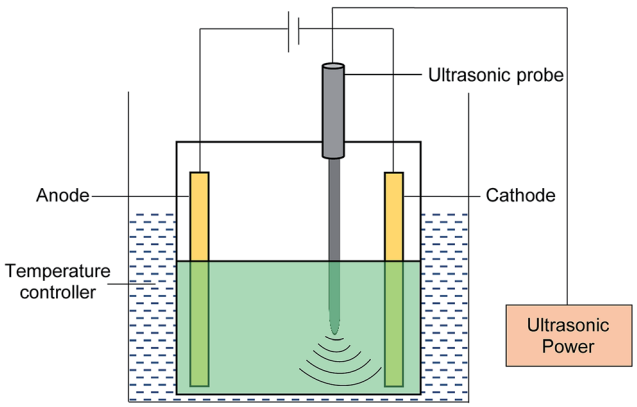

Fig. 1 Process assembly used for sonoelectrodeposition of Sn–Ni alloy coating.

developed by turning the ultrasound generator ON (t_{ON}) and OFF (t_{OFF}) periodically during deposition. The periodic modulation in mass transfer, due to the turning ON and OFF of the sonicator, allowed the growth of coatings with periodic modulation in their composition. In other words, periodic ON and OFF allowed the deposition to take place in multilayers. Sonoelectrodepositions have been accomplished by the combined effect of two driving forces: one is c.d., expressed in A dm^{-2}, and other one is p.d., expressed in W cm^{-2}. Here c.d. acts as the driving force for reduction of metal ions, and p.d. for modulating the mass transfer at EDL. The driving forces employed for deposition of monolayer and multilayer Sn–Ni alloy from the same optimized bath under different conditions of mass transfer process are shown schematically in Fig. 2,

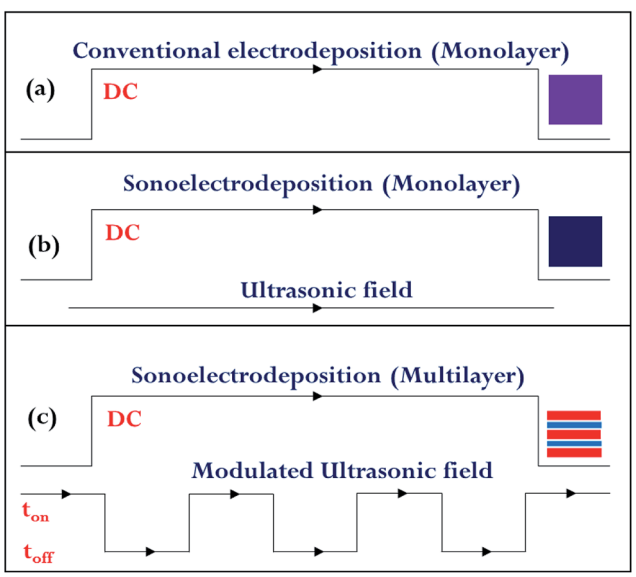

Fig. 2 Schematic representation of driving forces used for development of Sn–Ni alloy coatings from the same optimized bath along with deposit patterns on the right: (a) DC or constant current for conventional Sn–Ni alloy, (b) DC and ultrasonic field for sonoelectrodeposited Sn–Ni alloy (both monolayer), and (c) DC and pulsed ultrasound field for multilayer Sn–Ni alloy.

alongside their deposit patterns on the right-hand side in Fig. 2. The configuration of multilayer Sn–Ni coatings (sonoelectrodeposited) is conveniently represented as: $(Sn–Ni)_{1/2/n}$, where 1 and 2 indicate, respectively, ON time (t_{ON}) and OFF time (t_{OFF}) of sonication (in seconds), and 'n' represents the number of layers formed during total deposition time (*i.e.* 300 seconds).

2.2 Electrochemical measurements

All monolayer and multilayer Sn–Ni alloy coatings were deposited using the optimized bath (Table 1) for 5 minutes, for comparison purpose. After deposition, the coated surfaces were rinsed with distilled water several times, dried in hot air and desiccated until further testing. All electrochemical studies were made using a potentiostat/galvanostat (VersaSTAT3, Princeton Applied Research, USA) in a three-electrode configuration cell, using saturated calomel electrode (SCE) as reference electrode and platinum electrode as counter electrode. The corrosion tests were carried out on 1 cm^2 exposed surface area of the coatings in 5% NaCl at 298 K. Potentiodynamic polarization study was carried out with a potential ramp of ±250 mV around equilibrium potential at a scan rate of 1 mV s^{-1}. Electrochemical impedance spectroscopy (EIS) study was made using an AC signal of 10 mV amplitude, in a frequency range from 100 kHz to 20 mHz and the corresponding Nyquist plots were analysed. The corrosion rates (CRs) were expressed in mm $year^{-1}$, determined by the Tafel extrapolation method.[22]

2.3 Characterization

The topographical images of monolayer coatings and their composition were analysed using SEM (Zeiss Ultra 55, Germany, facilitated with EDX) and formation of multilayer coatings was confirmed using SEM (JSM-6380 LA, JEOL, Japan). The phase structures of the coatings for different conditions were analysed by X-ray diffraction (XRD, Rigaku Miniflex 600 machine), using Cu Kα ($\lambda = 1.5406$ Å) radiation, in continuous scan mode with a scan rate of 2° min^{-1}.

3. Results and discussion

3.1 Sonoelectrodeposition of Sn–Ni alloy coating

The Hull cell method was employed to determine the optimal electrolytic conditions for the deposition of bright, uniform and corrosion-resistant monolayer (Sn–Ni) alloy coatings over wide range of c.d. The experimental results revealed that under optimal condition of c.d. = 1.0 A dm^{-2}, the bath produced coating showing the least CR (16.63×10^{-2} mm $year^{-1}$), *i.e.* without ultrasonication. Keeping this c.d. as constant, the corrosion protection of Sn–Ni alloy coatings was tried to be enhanced by the ultrasound effect. Accordingly, monolayer Sn–Ni alloy coatings were deposited under different conditions of p.d. (*i.e.* at 0.6, 0.9 and 1.2 W cm^{-2}), and their corrosion performances were evaluated. The corrosion data are reported in Table 2. From the CR data, it may be noted that sonoelectrodeposited Sn–Ni alloy coatings are more corrosion resistant compared to the one deposited without ultrasonic field, *i.e.* p.d. = 0 W cm^{-2}, and the coating corresponding to 0.9 W cm^{-2}

Table 2 Corrosion data of sonoelectrodeposited Sn–Ni alloy coatings (monolayer) developed under different conditions of p.d., at constant c.d. = 1.0 A dm^{-2}

Ultrasonic p.d. (W cm^{-2})	t_{ON} (s)	wt% Ni	wt% Sn	$-E_{corr}$ (V *vs.* SCE)	i_{corr} (μA cm^{-2})	CR ($\times 10^{-2}$ mm $year^{-1}$)
0	300	60.9	39.1	0.5873	10.749	16.63
0.6	300	43.5	56.5	0.5768	5.362	9.38
0.9	300	42.2	57.8	0.5597	4.473	7.81
1.2	300	41.4	58.6	0.5766	4.741	8.27

exhibits the least CR (7.81×10^{-2} mm $year^{-1}$), which may be attributed to the relatively compact structure of the coatings as seen in Fig. 4. It should be noted that at high p.d. of 1.2 W cm^{-2}, the CR of the coating started increasing, and hence 0.9 W cm^{-2} has been taken as the optimal p.d. for pulsing of the sonication effect.

Further, it is important to note that wt% Sn in the deposit increased drastically when deposition was carried out under the effect of ultrasound. This drastic increase in wt% Sn is due to thinning of EDL (Nernst's diffusion layer) to a few microns in thickness.[19] The absolute value of this EDL thickness is actually determined by the geometry of the sonoelectrode and the ultrasonic p.d. The decrease of EDL thickness leads to an increase of limiting current density (i_L) required for the electrochemical process taking place at the electrode–electrolyte interface, and is described by the relation[23]

$$i_L = \frac{nFDC_B}{\delta} \quad (1)$$

where n is the number of transferred electrons, F the Faraday constant (96 500 C), D the diffusion coefficient, C_B the concentration and δ the thickness of EDL. Accordingly, the decreased thickness of EDL, due to the ultrasound effect, has increased the i_L for deposition of more noble metal (Sn) in the deposit, since $E^0_{Ni} = -0.25$ V and $E^0_{Sn} = -0.14$ V. Here, it is important to note that there occurs a drastic increase of Sn content of the alloy which is otherwise not possible in conventional Sn–Ni alloy plating. In conventional Sn–Ni alloy plating (developed using only DC) an anomalous type of codeposition takes place, where preferential deposition of Ni (less noble) compared to Sn (more noble) takes place. Thus, it may be inferred that the ultrasound effect has decreased the CR by increasing the Sn content in the alloy, which otherwise would not be possible due to the inherent limitation of anomalous type of codeposition in the proposed bath.

3.2 X-ray diffraction study

XRD patterns of sonoelectrodeposited Sn–Ni alloy coatings corresponding to different p.d. (from 0 W cm^{-2} to 1.2 W cm^{-2}) are shown in Fig. 3. It may be noted that the preferential orientations of Ni_3Sn_2 (214), Ni_3Sn_2 (413) and Ni_3Sn_2 (242) phases are favoured to exist in coatings developed both in the presence and absence of ultrasonic field, but Ni_3Sn_2 (302) (JCPDS card no. 65-1315) and Ni_3Sn (201) (JCPDS card no. 35-1362) reflections which are nickel-rich phases cease to exist under ultrasound field. There is the formation of a new peak of Ni_3Sn_2 (221) due to applied frequency of ultrasound p.d. The intensity of Ni_3Sn_2 (221) peak was found to increase with an increase in p.d. The Ni_3Sn_2 (111) phase is found to be characteristic of ultrasonication, and it observed to increase with p.d. as may be seen in Fig. 3. Another interesting observation is that there is a shift in the peak of Ni_3Sn_2 (112) under the ultrasonication effect. When the ultrasound frequency is applied, the wt% of Sn in the coatings is increased which is evident by the disappearance of the Ni_3Sn peak, being a nickel-rich phase. Hence it can be concluded that ultrasound frequency has a vital effect on composition, and hence on the phase structure of the coatings.

The corrosion protection and other physical properties of binary/ternary alloy coatings largely depend upon their phase composition. Hence any phase variation, affected by altering the deposition conditions, is of great value, and is a subject of materials research.[24] Further, experimental observation revealed that composition, phase structure and surface morphology of Sn–Ni alloy coatings largely depend on the ultrasound p.d. used. Hence, multilayer Sn–Ni alloy coatings have been fabricated on a nano/micrometric scale, with compositional modulation by pulsing the ultrasound at p.d. of

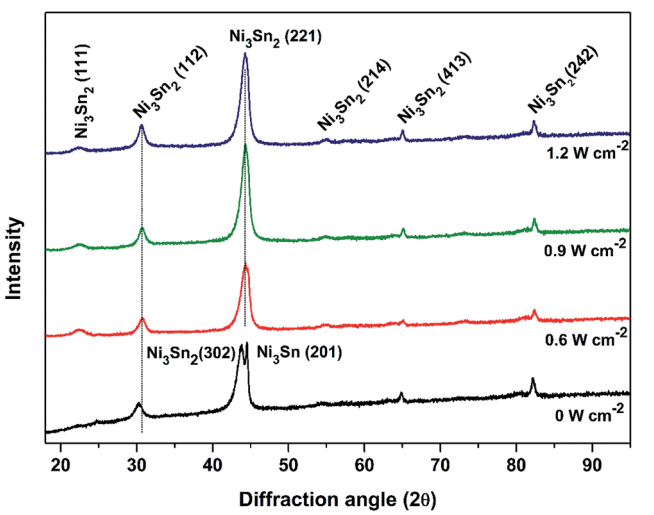

Fig. 3 XRD patterns showing change in crystallographic orientations of Sn–Ni alloy coatings deposited at different ultrasonic p.d., in relation to its monolayer coating without sonication, *i.e.* at 0 W cm^{-2}, deposited using the same bath at the same c.d. = 1.0 A dm^{-2}.

0.9 W cm^{-2} (optimal p.d. fixed) and 0 W cm^{-2} (as t_{ON} and t_{OFF}, respectively), keeping other parameters constant, *i.e.*, at optimal condition of c.d. = 1.0 A dm^{-2} and pH = 8.6.

3.3 SEM study of monolayer Sn–Ni alloy coating

The surface morphologies of Sn–Ni alloy coatings at different p.d. (*i.e.* at 0, 0.6, 0.9, 1.2 W cm^{-2}) are shown in Fig. 4. It may be noted that there are no significant changes in the surface morphology of the coatings with p.d., due to inherent nature of the Sn–Ni deposit.

Another interesting observation is that Sn–Ni coatings show characteristic micro-cracks on their surface as may be seen in Fig. 4. This may be attributed to hydrogen embrittlement as envisaged by Zhu *et al.*[25] According to which, during alloy deposition, hydrogen gas remains adsorbed on the surface due to low hydrogen overvoltage of Sn. The adsorbed hydrogen leads to the development of strain in the deposit, which subsequently leads to the formation of micro-cracks on the surface. Thus micro-cracks on the surface of Sn–Ni alloy coatings may be attributed to low hydrogen overvoltage of Sn.

3.4 Development of multilayer Sn–Ni alloy

The properties of multilayer coatings, including their corrosion behaviour, may often be improved substantially by increasing the number of layers (usually up to an optimal limit), without sacrificing the demarcation between each layer.[26] Generally, corrosion behaviour of CMMA coatings depends upon a variety of factors, such as choice of electrolyte, bilayer numbers and thickness of each layer.[24] Keeping this in view, multilayer Sn–Ni alloy coatings (having layer structure with alternate layers of alloy of two different compositions) have been developed, with different degree of layering. This is accomplished by setting the sonicator to turn ON and OFF at regular time intervals. Accordingly, multilayer Sn–Ni alloy coatings having 10, 30, 75, 100, 150 and 300 layers have been developed by programming the sonicator to go ON and OFF alternatively at 30, 10, 4, 3, 2 and 1 second intervals, respectively, and their corrosion behaviours have been studied. It should be noted that during periodic sonication, two layers of alloys of the same metals but of different composition (57.8 and 39.1 wt% Sn) were found to be formed alternatively as the sonicator probe go ON and OFF. This is evident from the EDS data reported in Table 2.

3.5 Corrosion study

3.5.1 Polarization study. The potentiodynamic polarization behaviour of multilayer Sn–Ni alloy coatings with different degrees of layering is shown in Fig. 5. It may be observed that the corrosion resistance of the deposits increased with the number of layers as evidenced by their corrosion data, reported in Table 3. The successive decrease of CR with the number of layers indicated that improved CRs are due to layered coating, having a distinct interface between layers. It is important to note that CRs of multilayer coatings decreased drastically with an increase in the number of layers up to 150 layers, and then increased, *i.e.* the multilayer coating having 150 layers, represented as $(Sn–Ni)_{2/2/150}$, shows the least CR. However, an

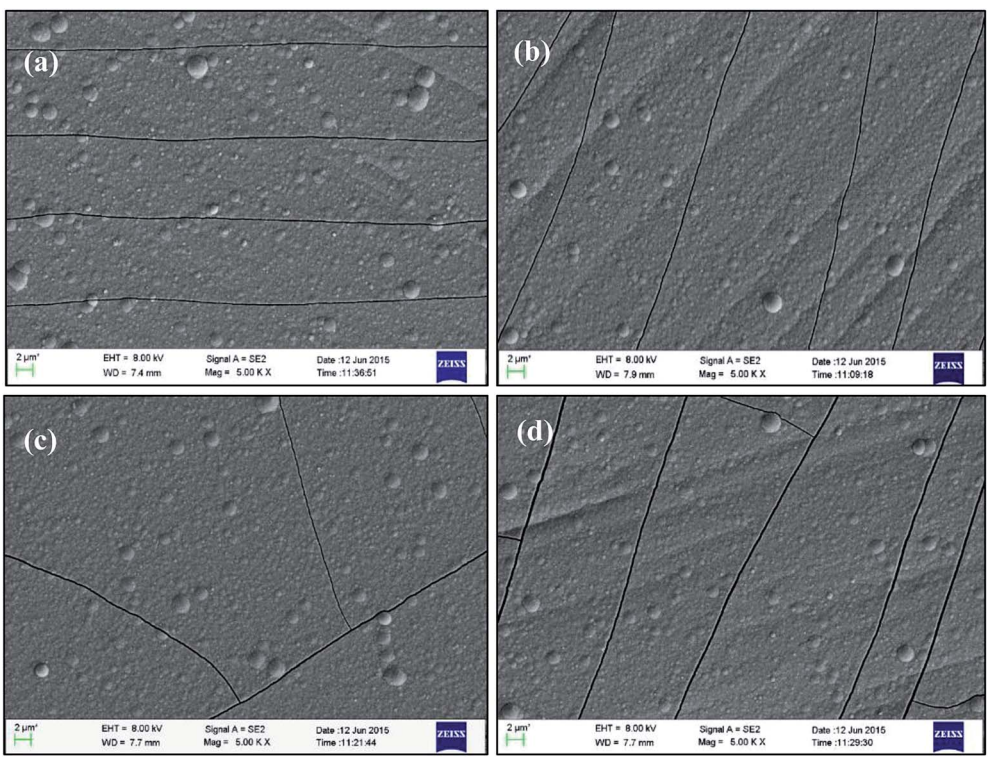

Fig. 4 SEM micrographs of Sn–Ni alloy coatings fabricated under different ultrasonic power densities: (a) 0 W cm^{-2}, (b) 0.6 W cm^{-2}, (c) 0.9 W cm^{-2} and (d) 1.2 W cm^{-2}.

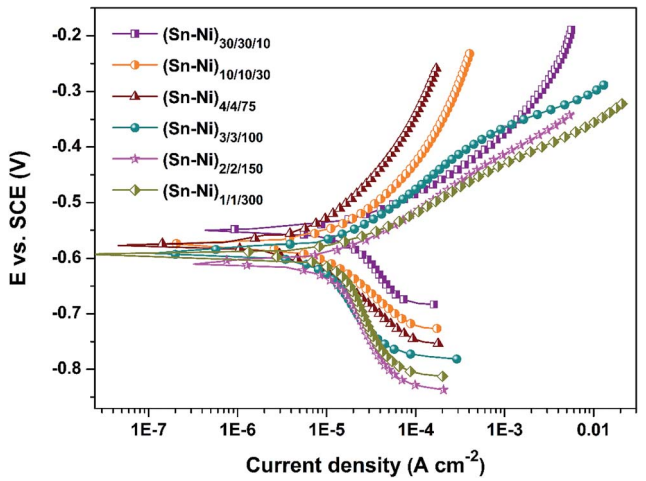

Fig. 5 Potentiodynamic polarization behaviour of sonoelectrodeposited multilayer Sn–Ni coatings, with different number of layers developed from same optimal bath at optimal c.d.

increase of CR at high degree of layering (at 300 layers) may be attributed to interlayer diffusion due to short relaxation time for metal ions, caused by rapidly changing ultrasound field. This may be explained as follows. During sonoelectrodeposition, metal ions (Sn^{2+} and Ni^{2+} ions) from the bulk electrolyte diffuse towards the cathode and discharge as metal atoms, and this process of mass transfer by diffusion is mainly controlled by the ultrasonic effect. As the number of layers increased, t_{ON} for metals to diffuse towards cathode is too small (1 s). Here it should be noted that total time for deposition remains the same (5 min). Thus at high degree of layering, there is not sufficient time for metal ions to relax (against diffusion under applied p.d.) and to deposit.[11–13] As a result, at high degree of layering no modulation in composition is likely to take place, and hence no improvement in CR was found. Based on the corrosion data, $(Sn–Ni)_{2/2/150}$ coating has been proposed as the optimal coating configuration, developed from the bath for highest performance against corrosion.

3.5.2 Electrochemical impedance spectroscopy study. EIS is a non-destructive method for studying the interfacial interaction of test materials very accurately. The ability of the technique to segregate various processes, *i.e.*, ohmic conduction, charge transfer, interfacial charging, mass transfer, *etc.*, makes it an elegant technique for electrochemical study.[27] In this technique, it is common to plot the data as imaginary impedance *versus* real impedance with provision to distinguish the polarization resistance (R_p) contribution from the solution resistance (R_s). These plots are often called Nyquist diagrams. Nyquist diagrams of Sn–Ni deposits with different number of layers were obtained, and are shown in Fig. 6.

The plots showed a depressed semicircle in the studied frequency range; in addition an increase of axial radius of the semicircle with number layers was found. Impedance signals clearly indicated that the charge transfer resistance (R_{ct}) has increased progressively with the number of layers before starting to decrease, *i.e.* at 300 layers. Thus impedance response of

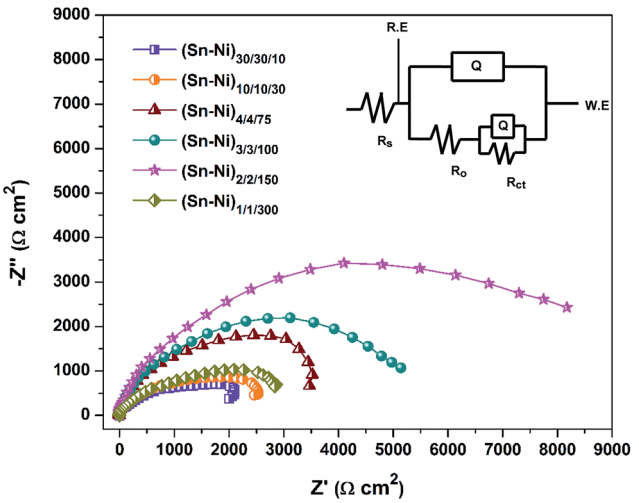

Fig. 6 EIS response of sonoelectrodeposited multilayer Sn–Ni alloy coatings, with different number of layers developed from the same optimal bath at optimal c.d.

Table 3 Corrosion data for multilayer Sn–Ni alloy coatings deposited from same bath keeping other parameters constant, like c.d. = 1.0 A dm^{-2}, ultrasonic p.d. = 0.9 W cm^{-2}

Multilayer Sn–Ni alloy coating configuration	Total time taken for deposition, t = 300 s		No. of layers formed	$-E_{corr}$ (V *vs.* SCE)	i_{corr} (μA cm^{-2})	CR ($\times 10^{-2}$ mm $year^{-1}$)
	t_{ON} (s)	t_{OFF} (s)				
$(Sn–Ni)_{30/30/10}$	30	30	10	0.610	3.544	6.18
$(Sn–Ni)_{10/10/30}$	10	10	30	0.589	3.113	5.43
$(Sn–Ni)_{4/4/75}$	4	4	75	0.575	2.384	4.16
$(Sn–Ni)_{3/3/100}$	3	3	100	0.591	1.622	2.83
$(Sn–Ni)_{2/2/150}$	2	2	150	0.610	1.128	1.97
$(Sn–Ni)_{1/1/300}$	1	1	300	0.591	2.621	4.57
Monolayer Sn–Ni alloy						
$(Sn–Ni)_{1.0}$ A dm^{-2}			Monolayer	0.587	10.749	16.63
$(Sn–Ni)_{1.0/0.9}$ W cm^{-2}			Monolayer	0.559	4.473	7.81

$(Sn–Ni)_{2/2/150}$, characterized by very high polarization resistance R_p, indicates that this coating configuration is more stable than the other coatings, in compliance with Tafel plots shown in Fig. 5. An increase of capacitive reactance with number of layers, shown in Fig. 6, demonstrated that CR of multilayer coatings decreases with an increase in number of layers (only up to 150), and then further increased. Thus the EIS response of $(Sn–Ni)_{2/2/150}$ alloy, characterized by high polarization resistance R_p, indicates that this particular coating is electrochemically more stable than the other coatings. The electrochemical equivalent circuit corresponding to $(Sn–Ni)_{2/2/150}$ has been simulated, and is shown in the inset of Fig. 6, where R_s is solution resistance, R_o is pore resistance, R_{ct} is charge transfer resistance and Q is capacitance of EDL. Here R_o refers to the resistance of ion conducting paths developed in the coating due the presence of micro-cracks or due to the deformation of the coating at the topmost layer of the CMMA coating. These paths are physical pores filled with electrolyte, *i.e.*, corrosion medium. Since in multilayer coating the pore or the cracks on the top layer will not reach up to the substrate (confirmed from the SEM cross-sectional analysis) due to the presence of several other layers of different composition below the top layer, the pore/crack will reach only up to a few lower layers.[28] A good agreement was found between experimental and simulated EIS response, corresponding to $(Sn–Ni)_{2/2/150}$ coating. Hence it may be concluded that highest corrosion protection of $(Sn–Ni)_{2/2/150}$ coating is mainly attributed to charge transfer resistance (R_{ct}).

3.5.3 Comparison of monolayer and multilayer Sn–Ni alloy coatings. The decrease of CRs when coating is changed from conventional monolayer to sonoelectrodeposited monolayer, and then to multilayer (ultrasound-assisted) coating may be confirmed by the data summarized in Table 3. The corrosion behaviours of monolayer (with and without sonication effect) and multilayer Sn–Ni alloy coatings (all under optimal conditions) from the same bath for the same duration are shown comparatively through Nyquist plots, with corresponding potentiodynamic polarization curves, in Fig. 7a and b.

A considerable decrease of CRs was observed for Sn–Ni CMMA coating compared to both its monolayer coatings, as may be seen in Table 3. Similarly, a drastic increase of R_p was found in the case of sonoelectrodeposited multilayer coatings, as shown in Fig. 6. Thus from corrosion data it may concluded that, under optimal conditions, $(Sn–Ni)_{2/2/150}$ is about 4 times more corrosion resistant (CR = 1.97×10^{-2} mm year^{-1}) than sonoelectrodeposited coating (CR = 7.81×10^{-2} mm year^{-1}) and 8.4 times more corrosion resistant than conventional coating with no ultrasound pulse (CR = 16.63×10^{-2} mm year^{-1}) developed from the same bath.

3.6 SEM study of multilayer Sn–Ni alloy coating

The SEM image of a cross-sectional view of multilayer Sn–Ni coating with 10 layers, having alternately different composition (5 each), represented as $(Sn–Ni)_{30/30/10}$, is shown in Fig. 8. Clear demarcations on the cross section of the coating evidence the formation of layers, due to periodic pulsing of p.d. during deposition. In other words, periodic modulation of ultrasound p.d. during deposition allowed the formation of interfaces, separating two layers of alloys having different composition. It

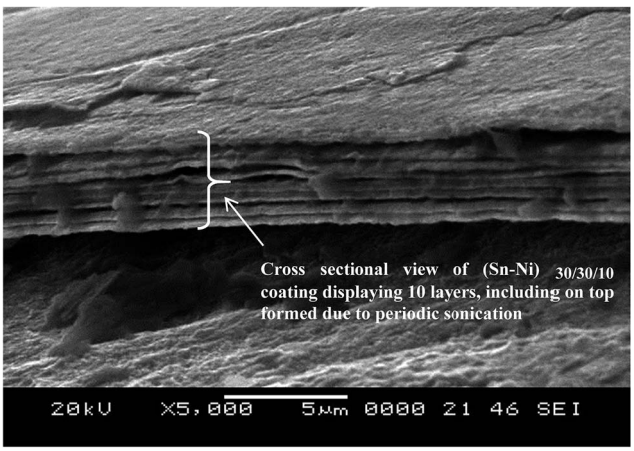

Fig. 8 SEM cross-sectional view of multilayer Sn–Ni coating, represented as $(Sn–Ni)_{30/30/10}$ displaying 10 layers, having alternately different composition.

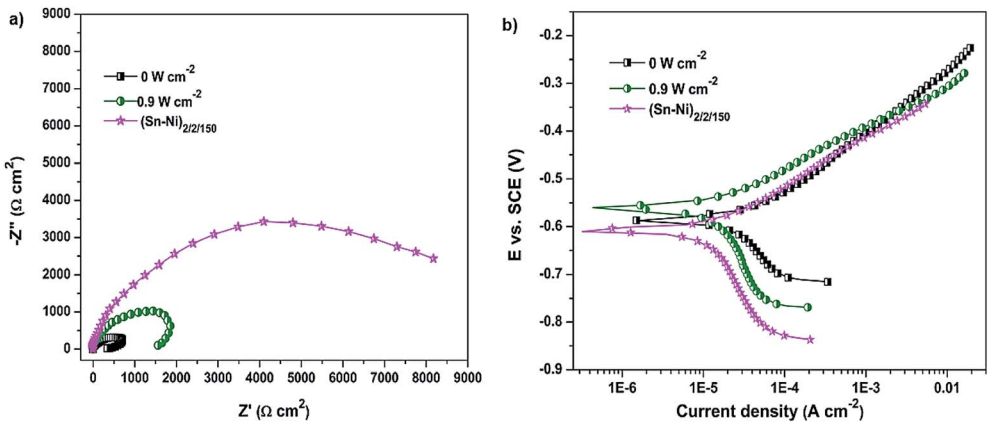

Fig. 7 Comparison of (a) Nyquist plots and (b) potentiodynamic polarization curves of monolayer and multilayer Sn–Ni alloy coatings developed under optimal conditions, from the same bath for the same duration.

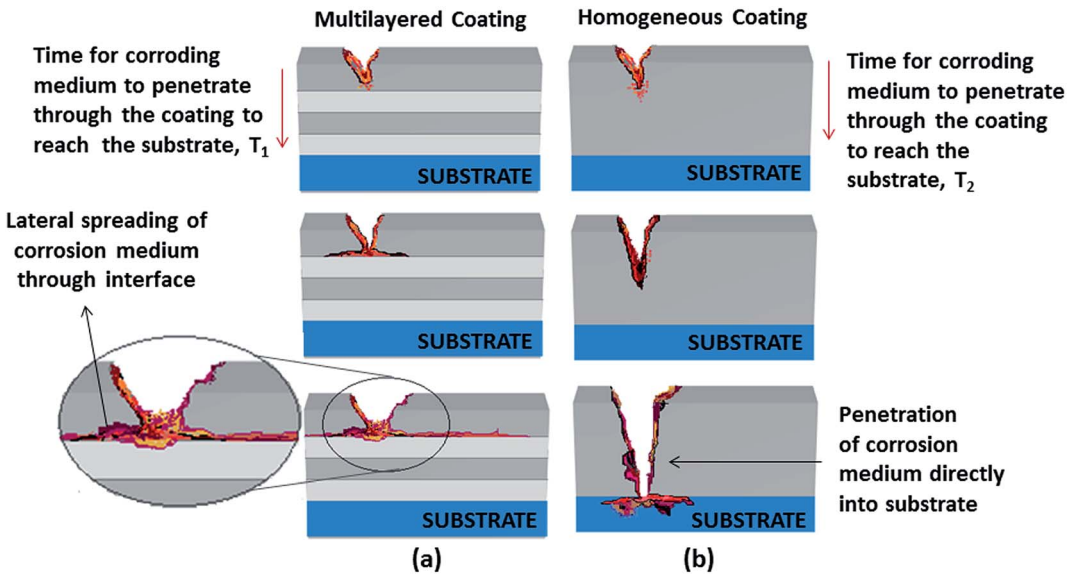

Fig. 9 Schematic diagram representing the increased corrosion protection of multilayer coatings compared to counterpart monolayer coatings: (a) corrosion medium spreads laterally at the interface between layers and the corrosion is reduced, and (b) corrosion medium attacks directly to reach the substrate faster through monolayer coating.

may further be noted that for a total of 5 min duration, a coating about 5 μm (micron) in thickness has developed on the substrate, as may be seen in Fig. 8.

Therefore, it may be concluded that for the multilayer Sn–Ni coating under optimal condition, *i.e.* with $(Sn–Ni)_{2/2/150}$ configuration, the thickness of each layer is found to be in the range of 33 nm. Thus improved corrosion protection of multilayer Sn–Ni alloy coating is due to nano/micrometric layering of alloys effected by periodic pulsing of the sonicator probe.

3.7 Mechanism of corrosion

The efficacy of corrosion protection of the mild steel substrate by multilayer coatings in contrast to monolayer alloy coatings can be convincingly explained by a pictorial representation as shown in Fig. 9. This mechanism is attributed by the selective dissolution of several layers with alternating compositions.[29] In Fig. 9 it should be noted that Sn–Ni multilayer coating is represented by 4 layers of alloys, where 2 layers of alloys have one composition (grey colour) which is alternated by 2 layers of alloys with a different composition (light blue colour), giving better corrosion protection to the substrate than its counterpart monolayer alloy coating of the same thickness. When the layered alloy coating comes in contact with the corrosion medium, the top layer is exposed directly and gets corroded first. The layers present beneath are safe until the breakdown of the topmost layer occurs. As the corrosive agent penetrates the lower layers the corrosion product spreads laterally at the interface as shown in Fig. 9a. Once that layer breaks down, the lower layer gets exposed to the corrosive medium and this process repeats layer after layer. Thus if the number of layers is more, the corrosive agent takes a longer time to penetrate through the layers and then into the substrate. Hence, this process blocks or extends the path of the corrosive agent.[30,31] However, at high degree of layering, *i.e.* at 300 layers, the corrosion rate was found to be more since no modulation in the composition of alloys will take place, as explained in Section 3.5.1. In the case of monolayers (both conventional and sonoelectrodeposited Sn–Ni alloy), corrosion takes place continuously to reach the substrate directly as shown in Fig. 9b. Thus the observed decrease of CR with an increase of number of layers may be attributed to increased number of layers, or interfaces separating alloys of different composition. Here, the word 'interface' is used in the sense of phase boundary separating alloys of different composition, but of the same metals. Therefore, as the number of layers increases, the total surface area of phase boundary (under given area of the coating) increases. This allows the corrosion medium to spread laterally more than to filter directly into the substrate, as in monolayer coating.[32,33] Thus it may also be concluded from Fig. 9 that the total time required for the corroding medium to reach the substrate by penetrating through the multilayer coating (T_1) is much greater than that through the monolayer coating (T_2), *i.e.* $T_1 \gg T_2$.

4. Conclusions

Multilayer Sn–Ni alloy coatings have been developed on MS, using the ultrasonic effect as a tool for modulating the mass transport process at EDL during deposition. The following conclusions are drawn.

(1) Ultrasound effect decreases the CR of Sn–Ni alloy coatings by increasing the Sn content of the alloy, which is otherwise not possible due to the inherent limitation of anomalous type of codeposition followed using the proposed bath.

(2) Multilayer Sn–Ni alloy coatings, having layers on a micrometric scale with alternately changing composition,

were fabricated by turning the ultrasonicator ON and OFF as required, keeping the c.d. constant.

(3) Under optimal conditions $(Sn–Ni)_{2/2/150}$ is about 4 times more corrosion resistant (CR = 1.97×10^{-2} mm year^{-1}) than sonoelectrodeposited coating (CR = 7.81×10^{-2} mm year^{-1}), and 8.4 times more corrosion resistant than conventional coating with no ultrasound effect (CR = 16.63×10^{-2} mm year^{-1}), developed from the same bath for the same time.

(4) The improved corrosion protection of multilayer Sn–Ni alloy coatings is due to nano/micrometric layering of alloys of different composition (57.8 and 39.1 wt% Sn) effected by periodic sonication.

(5) Improved corrosion protection of multilayer Sn–Ni alloy coatings was attributed to the formation of a greater number of layers, separating the layers of alloys of the same metal but of different composition, phase structure and surface morphology, supported by EDS, XRD and SEM study.

Acknowledgements

Ms Sandhya Shetty acknowledges the National Institute of Technology Karnataka (NITK), Surathkal for financial assistance in the form of an institute fellowship and infrastructure to carry out the present work.

References

1 V. Thangaraj, N. Eliaz and A. C. Hegde, *J. Appl. Electrochem.*, 2009, **39**, 339–345.
2 G. Wilcox and D. Gabe, *Corros. Sci.*, 1993, **35**, 1251–1258.
3 N. Kanani, *Electroplating: basic principles, processes and practice*, Elsevier, 2004.
4 S. Yogesha and A. C. Hegde, *J. Met., Mater. Miner.*, 2011, **21**, 83–92.
5 A. Haseeb, J.-P. Celis and J. Roos, *J. Electrochem. Soc.*, 1994, **141**, 230–237.
6 U. Cohen, F. Koch and R. Sard, *J. Electrochem. Soc.*, 1983, **130**, 1987–1995.
7 J. Yahalom and O. Zadok, *J. Mater. Sci.*, 1987, **22**, 499–503.
8 T. J. Mason and E. D. Cordemans, *Chem. Eng. Res. Des.*, 1996, **74**, 511–516.
9 T. J. Mason, *Molecules*, 2009, **14**, 4284–4299.
10 S. Yogesha and A. C. Hegde, *Trans. Inst. Met. Finish.*, 2010, **88**, 317–323.
11 S. Yogesha and A. C. Hegde, *Anti-Corros. Methods Mater.*, 2011, **58**, 84–89.
12 S. Yogesha and A. C. Hegde, *J. Mater. Process. Technol.*, 2011, **211**, 1409–1415.
13 K. Venkatakrishna and A. C. Hegde, *Mater. Manuf. Processes*, 2011, **26**, 29–36.
14 G. Pavithra and A. C. Hegde, *Appl. Surf. Sci.*, 2012, **258**, 6884–6890.
15 Y. Ullal and A. C. Hegde, *Appl. Phys. A: Mater. Sci. Process.*, 2014, **116**, 1587–1594.
16 D. Peters, *J. Mater. Chem.*, 1996, **6**, 1605–1618.
17 C. E. Banks and R. G. Compton, *Electroanalysis*, 2003, **15**, 329–346.
18 J. C. Eklund, F. Marken, D. N. Waller and R. G. Compton, *Electrochim. Acta*, 1996, **41**, 1541–1547.
19 F. J. Del Campo, B. Coles, F. Marken, R. Compton and E. Cordemans, *Ultrason. Sonochem.*, 1999, **6**, 189–197.
20 B. Subramanian, S. Mohan and S. Jayakrishnan, *J. Appl. Electrochem.*, 2007, **37**, 219–224.
21 S. Refaey, F. Taha and T. Hasanin, *Electrochim. Acta*, 2006, **51**, 2942–2948.
22 D. A. Jones, *Principles and prevention of corrosion*, Macmillan, 1992.
23 C. M. Brett and A. M. O. Brett, *Electrochemistry: principles, methods, and applications*, Oxford university press, 1993.
24 P. Ganesan, S. P. Kumaraguru and B. N. Popov, *Surf. Coat. Technol.*, 2007, **201**, 7896–7904.
25 L. Zhu, O. Younes, N. Ashkenasy, Y. Shacham-Diamand and E. Gileadi, *Appl. Surf. Sci.*, 2002, **200**, 1–14.
26 S. Yogesha, R. S. Bhat, K. Venkatakrishna, G. Pavithra, Y. Ullal and A. C. Hegde, *Synth. React. Inorg., Met.-Org., Nano-Met. Chem.*, 2011, **41**, 65–71.
27 X.-Z. R. Yuan, C. Song, H. Wang and J. Zhang, *Electrochemical impedance spectroscopy in PEM fuel cells: fundamentals and applications*, Springer Science & Business Media, 2009.
28 L. Elias and A. C. Hegde, *Surf. Coat. Technol.*, 2015, **283**, 61–69.
29 J.-Y. Fei and G. D. Wilcox, *Electrochim. Acta*, 2005, **50**, 2693–2698.
30 P. Leisner, C. B. Nielsen, P. T. Tang, T. C. Dörge and P. Møller, *J. Mater. Process. Technol.*, 1996, **58**, 39–44.
31 K. Venkatakrishna and A. C. Hegde, *J. Appl. Electrochem.*, 2010, **40**, 2051–2059.
32 L. Elias, U. K. Bhat and A. C. Hegde, *RSC Adv.*, 2016, **6**, 34005–34013.
33 L. A. Dobrzanski, K. Lukaszkowicz, A. Zarychta and L. Cunha, *J. Mater. Process. Technol.*, 2005, **164–165**, 816–821.